

THE PERIOD CHANGES OF YY ERIDANI

CHUN-HWEY KIM AND JANG HAE JEONG

Department of Astronomy and Space Science, Chungbuk National University, San 48, Gaeshindong, Cheongju 360-763,
Chungbuk, Korea

Electronic mail: kimch@astro.chungbuk.ac.kr

OSMAN DEMIRCAN AND ZEKERIYA MÜYESSEROĞLU

Ankara University Observatory, Department of Astronomy, Science Faculty, Tandogan, Ankara, Turkey

Electronic mail: demircan@dione.astro.science.ankara.edu.tr

EDWIN BUDDING

Central Institute of Technology, P.O. Box 40740, Wellington, New Zealand, Carter Observatory, P.O. Box 2909, Wellington,
New Zealand

Electronic mail: budding@ee.cit.ac.nz

Received 1997 April 24; revised 1997 August 1; accepted 1997 August 26

ABSTRACT

18 new times of minimum light for YY Eri were determined from relatively new or unpublished photoelectric observations from Korea, New Zealand, and Turkey, and added to a collection of all other times of minima available to us. These data were then intensively analyzed, by reference to an O–C diagram, to deduce the general form of period variation for YY Eri. The O–C diagram could be either of quasi-sinusoidal form superposed on an upward parabola, or a set of abrupt changes. If abrupt changes, they appear to have occurred alternately in a pattern of two increases following one decrease. This may be an indication of underlying sinusoidal variations, rather than real sudden changes of period, associated with sudden mass ejections in the system. An upward parabolic O–C diagram corresponds to a secular period increase, usually interpreted as mass transfer from the less to the more massive component. The sinusoidal character suggests an unseen third body, or cyclic strong magnetic activity on at least one of the component stars. The long term sinusoidal light level variation is supported by cyclical magnetic activity effects in the orbital period. However, the existence of a third body cannot be ruled out by the present data. © 1997 *American Astronomical Society*. [S0004-6256(97)01512-4]

1. INTRODUCTION

The study of period changes of eclipsing variable stars provides important and direct clues in understanding certain astrophysically interesting topics, such as: the internal structures of the stars, tests of the theory of general relativity, the three-body problem, mass transfer from one component to the other, mass loss from one (or both) component(s), and magnetic activities of the stars. This study has been usually based on the relatively simple O–C diagram, formed from observed times of (eclipse) minimum light (O), minus those calculated from an ephemeris (C), plotted against time (or the number of revolutions).

A quasi-sinusoidal (O–C) variation could be produced by at least three physical causes: (a) apsidal motion of an elliptic orbit, (b) light time effect due to a third body, or (c) cyclic changes of magnetic activity of one (or both) of the component stars. From the behavior of the (O–C) residuals for both primary and secondary minima, apsidal motion can be easily discerned from other mechanisms. Thus, with apsidal motion, the (O–C) residuals for primary epochs are nearly 180° out of phase from those of corresponding secondary minima. The (O–C) residuals at both minima resulting from the other cited effects would be in phase with each other.

With the nonapsidal motion effects, however, it would be quite difficult, in general, using only the (O–C) diagram, to determine which mechanism would be more appropriate to explain quasi-sinusoidal period changes. Other observables, which can discriminate between rival theories, must then be pursued [see, for example, the papers of Kalimeris *et al.* (1994) and Demircan *et al.* (1994) for the case of AB And]. This problem provides one focus for the present paper.

An (O–C) diagram with a parabolic variation points to continuous mass transfer from one component to the other, or steady isotropic mass loss with high ejection velocity, as likely causes (Huang 1963; Batten 1973). If the (O–C) diagram shows sudden period jumps, however, and the period between two consecutive jumps is constant, then a plausible mechanism involves occasional mass ejections from the components (Wood 1950).

The eclipsing binary YY Eri (BD–10:858, $P=0^d.321$, $S_p=G5$) shows a W UMa type light curve, implying a contact or near-contact physical configuration (cf. Budding *et al.* 1997, hereafter referred to as Paper I). The primary eclipse is that of the smaller star, indicating the “W-type” arrangement (Binnendijk 1965, 1970). Since the first photoelectric observations of Cillie (1951), YY Eri has been monitored

Table 1. The observed times of minima of YY Eri.

Time of Minima (JD Hel 2440000+)	Filter	Weighted Mean (JD Hel 2440000+)	Type	Note*	Time of Minima (JD Hel 2440000+)	Filter	Weighted Mean (JD Hel 2440000+)	Type	Note*
5709.9485 ± 3	V	5709.9487 ± 3	I	KAO	8262.3127 ± 9	B	8262.3127 ± 8	I	AUO
.9487 ± 2	B				.3128 ± 13	V			
.9491 ± 5	U				8268.2595 ± 5	B	8268.2594 ± 4	II	AUO
5710.1099 ± 1	V	5710.1101 ± 2	II	KAO	.2593 ± 8	V			
.1102 ± 1	B				8277.2615 ± 2	B	8277.2616 ± 2	II	AUO
.1102 ± 3	U				.2618 ± 4	V			
5726.0235 ± 9	U	5726.0239 ± 6	I	KAO	8646.3409 ± 6	U	8646.3410 ± 4	II	AUO
.0238 ± 4	V				.3402 ± 7	B			
.0240 ± 5	B				.3421 ± 7	V			
5740.0096 ± 2	B	5740.0097 ± 2	II	KAO	8654.2152 ± 16	U	8654.2169 ± 4	I	AUO
.0097 ± 2	V				.2168 ± 5	B			
.0097 ± 2	U				.2176 ± 9	V			
7128.3934 ± 6	B	7128.3933 ± 3	I	AUO	8935.5272 ± 10	U	8935.5275 ± 4	I	AUO
.3932 ± 4	V				.5265 ± 5	B			
7530.4227 ± 7	B	7530.4227 ± 7	II	AUO	.5289 ± 6	V			
7537.3352 ± 9	U	7537.3346 ± 4	I	AUO	8952.4061 ± 7	B	8952.4061 ± 7	II	AUO
.3369 ± 10	B				8978.2862 ± 5	U	8978.2861 ± 3	I	AUO
.3336 ± 6	V				.2865 ± 5	B			
7862.3696 ± 11	B	7862.3702 ± 4	I	AUO	.2856 ± 4	V			
.3703 ± 4	V				8980.3754 ± 8	U	8980.3760 ± 3	II	AUO
7918.3099 ± 9	U	7918.3099 ± 4	I	AUO	.3757 ± 5	B			
.3099 ± 4	B				.3765 ± 6	V			

*KAO=Korean Astronomical Observatory, AUO=Ankara University Observatory

and studied by Huruwata *et al.* (1953), Kwee (1958), Purgathofer & Purgathofer (1960), Bhattacharyya (1967), Budding (1983), Eaton (1986), Müyesseröglü *et al.* (1990), Maceroni *et al.* (1994) and Hobart *et al.* (1994), as well as in Paper I. Spectroscopic observations were made by Struve (1947) and Nesci *et al.* (1986).

Some of the foregoing investigators reported a variable orbital period for YY Eri. Kwee (1958) found the period had increased since the earliest observations, which was confirmed by Purgathofer & Purgathofer (1960). The Purgathofers noted a quasi-parabolic form to the (O–C) curve, though Bhattacharyya (1967) obtained quasi-sinusoidal changes of period from mid-1930 to mid-1960. Strauss (1976) also noticed nonlinear changes in the period, while Budding (1983) remarked that such variations might be linked with intrinsic variations of the system, as evidenced by the spectroscopic irregularities (Struve 1947) and polarization variability (Oshchepkov 1973).

Kim (1992) found the orbital period to have varied sinusoidally with the small amplitude of about 0^d.003 over ~24 year cycles, since at least around 1950. He suggested that these changes were due to either a light-time effect from a hypothetical third body, or asymmetries of the light curves arising from stellar “activity.” More recently, however, Maceroni & van’t Veer (1994) showed that carefully timed

minima of YY Eri have deviated from Kim’s sine term ephemeris, implying some complexity to the period changes.

2. TIMES OF MINIMA AND (O–C) DIAGRAM

YY Eri was separately observed at three places: the Korean Astronomical Observatory outstation at Sobaeksan (Kim 1992) in 1983–1984 (six nights), the Black Birch Outstation of Carter Observatory (Budding 1983) in 1983 (five nights) and 1987 (seven nights), and the Ankara University Observatory (Müyesseröglü *et al.* 1990) in 1988 (7 nights) and early 1989 (5 nights). More details of these observations were given in Paper I. From the observations of the Korean Astronomical and the Ankara University Observatory a total of eighteen new times of minima have been determined using the method of Kwee & van Woerden (1956) (hereafter KW). These are listed in Table 1. Two times of minimum light obtained from the observations at the Black Birch Observatory were separately presented in Paper I.

We subsequently collected a total of 495 times of minima, from which all known photoelectric and CCD ones, and some selected visual and photographic observations are listed in Table 2. The included visual and photographic data are previous to the photoelectric minima.

TABLE 2. Times of minima of YY Eri used in our analysis.

Time of Minima ^a (JD 2400000+)	Cycles	(O - C) ^b	(O - C) ^c	Ty.	Me.	Ref.
26334.3670	-22654	0.0224	0.0041	I	VI	Jensch (1934)
27119.312	-20212.5	0.0344	0.0176	II	PG	Trembolt (1933)
27364.440	-19450	0.0215	0.0052	I	PG	Prager (1941)
27392.4119	-19363	0.0232	0.0070	I	VI	Jensch (1934)
28535.323	-15808	0.0153	0.0012	I	VI	Lause (1934)
28538.213	-15799	0.0118	-0.0022	I	VI	Lause (1934)
28573.255	-15690	0.0107	-0.0032	I	VI	Lause (1934)
28573.2556	-15690	0.0113	-0.0026	I	VI	Lause (1934)
28579.367	-15671	0.0143	0.0003	I	VI	Lause (1934)
28621.8030	-15539	0.0128	-0.0011	I	PG	Bodokia (1938)
33574.6001	-133.5	0.0000	-0.0044	II	PE	Cillie (1951)
33580.5480	-115	0.0002	-0.0042	I	PE	Cillie (1951)
33587.4606	-93.5	0.0007	-0.0038	II	PE	Cillie (1951)
33599.5163	-56	0.0003	-0.0041	I	PE	Cillie (1951)
33611.5724	-18.5	0.0002	-0.0041	II	PE	Cillie (1951)
33617.5197	0	-0.0001	-0.0045	I	PE	Cillie (1951)
33619.4487	6	-0.0001	-0.0045	I	PE	Cillie (1951)
33624.4318	21.5	-0.0002	-0.0046	II	PE	Cillie (1951)
33626.5215	28	-0.0002	-0.0046	I	PE	Cillie (1951)
33630.3800	40	0.0003	-0.0040	I	PE	Cillie (1951)
33631.3438	43	-0.0004	-0.0047	I	PE	Cillie (1951)
33631.5050	43.5	0.0001	-0.0043	II	PE	Cillie (1951)
33632.4692	46.5	-0.0002	-0.0045	II	PE	Cillie (1951)
33633.4337	49.5	-0.0002	-0.0045	II	PE	Cillie (1951)
33989.1691*	1156	-0.0004	-0.0040	I	PE	Huruhata <i>et al.</i> (1953)
34004.1188*	1202.5	-0.0002	-0.0039	II	PE	Huruhata <i>et al.</i> (1953)
34647.59263	3204	-0.0011	-0.0035	I	PE	Kwee (1958)
36540.88519	9093	0.0003	0.0015	I	PE	Purgathofer (1960)
36541.6889*	9095.5	0.0003	0.0015	II	PE	Purgathofer (1960)
36541.84937	9096	0.0000	0.0012	I	PE	Purgathofer (1960)
36542.81386	9099	0.0000	0.0012	I	PE	Purgathofer (1960)
36543.77838	9102	0.0000	0.0012	I	PE	Purgathofer (1960)
38413.281	14917	0.0022	0.0069	I	PE	Pohl & Kizilirmak (1966)
39120.2503	17116	0.0013	0.0074	I	PE	Bhattacharyya (1967)
39124.1085	17128	0.0016	0.0077	I	PE	Bhattacharyya (1967)
39162.2058	17246.5	0.0015	0.0077	II	PE	Bhattacharyya (1967)
39165.0999	17255.5	0.0022	0.0084	II	PE	Bhattacharyya (1967)
39165.2596	17256	0.0011	0.0073	I	PE	Bhattacharyya (1967)
39166.2241	17259	0.0011	0.0073	I	PE	Bhattacharyya (1967)
39167.1886	17262	0.0012	0.0074	I	PE	Bhattacharyya (1967)
39181.1742	17305.5	0.0017	0.0079	II	PE	Bhattacharyya (1967)
39187.1216	17324	0.0014	0.0076	I	PE	Bhattacharyya (1967)
40201.4399	20479	-0.0009	0.0073	I	PE	Pohl & Kizilirmak (1970)
40868.5418	22554	-0.0036	0.0058	I	PE	Kizilirmak & Pohl (1971)
41680.3167	25079	-0.0066	0.0043	I	PE	Kizilirmak & Pohl (1974)
41928.5121	25851	-0.0063	0.0051	I	PE	Kizilirmak & Pohl (1974)
42032.0335	26173	-0.0067	0.0050	I	PE	Strauss (1976)
43118.8477*	29553.5	-0.0104	0.0033	II	PE	Eaton (1986)
43119.8128*	29556.5	-0.0098	0.0039	II	PE	Eaton (1986)
43123.8303	29569	-0.0110	0.0027	I	PE	Eaton (1986)
43124.7948*	29572	-0.0110	0.0027	I	PE	Eaton (1986)
43398.5500	30423.5	-0.0098	0.0044	II	PE	Ebersberger <i>et al.</i> (1978)
44636.309	34273.5	-0.0113	0.0054	II	PE	Diethelm (1982)
44996.7034	35394.5	-0.0141	0.0032	II	PE	Skillman (1982)

We examined all minima showing large deviations from the general behavior of the (O-C) curve of YY Eri and, where possible, redetermined new minima from original data using the KW method. Among the minima in Table 2, one primary minimum (JD 2433989.1691) was redetermined using the individual observations of Huruhata *et al.* (1953). We found a difference of some 0^d.0014 from the original timing. Another pair of secondary minima were deduced from Huruhata *et al.*'s individual observations, as well as those of the Purgathofers' (1960), as JD 2434004.1188 and JD

2436541.6889. Three timings were also obtained from Eaton's (1986) observations, viz. JD 2443118.8477, JD 2443119.8128, and JD 2443123.8303, as indicated in Table 2.

All 495 times of minima were used to produce the (O-C) diagram of YY Eri drawn in Fig. 1. For this diagram we used the light elements of the Purgathofers (1960):

$$\text{Min I} = \text{JD } 2433617.51983 + 0^{\text{d}}.321496212E. \quad (1)$$

The (O-C) values obtained by Eq. (1) are given in the

TABLE 2. (continued)

Time of Minima ^a (JD 2400000+)	Cycles	(O - C) ^b	(O - C) ^c	Ty.	Me.	Ref.
45356.9456	36515	-0.0084	0.0096	I	PE	Budding (1983)
45709.9487	37613	-0.0082	0.0105	I	PE	This Paper
45710.1101	37613.5	-0.0075	0.0111	II	PE	This Paper
45726.0239	37663	-0.0078	0.0109	I	PE	This Paper
45740.0096	37706.5	-0.0071	0.0116	II	PE	This Paper
45757.8529	37762	-0.0069	0.0119	I	PE	Budding <i>et al.</i> (1997)
46774.7457	40925	-0.0066	0.0141	I	PEV	Hobart <i>et al.</i> (1993)
46774.9090	40925.5	-0.0041	0.0166	II	PEV	Hobart <i>et al.</i> (1993)
46778.7648	40937.5	-0.0062	0.0145	II	PEV	Hobart <i>et al.</i> (1993)
46798.6983	40999.5	-0.0055	0.0152	II	PEV	Hobart <i>et al.</i> (1993)
46799.6610	41002.5	-0.0073	0.0135	II	PEV	Hobart <i>et al.</i> (1993)
46818.6288	41061.5	-0.0077	0.0130	II	PEV	Hobart <i>et al.</i> (1993)
47080.1707	41875	-0.0030	0.0182	I	PE	Budding <i>et al.</i> (1997)
47128.3933	42025	-0.0048	0.0165	I	PE	This Paper
47458.8953	43053	-0.0009	0.0210	I	PEV	Hobart <i>et al.</i> (1993)
47459.8550	43056	-0.0057	0.0162	I	PEV	Hobart <i>et al.</i> (1993)
47530.4227	43275.5	-0.0065	0.0157	II	PE	This Paper
47537.3346	43297	-0.0067	0.0154	I	PE	This Paper
47862.3702	44308	-0.0038	0.0190	I	PE	This Paper
47918.3099	44482	-0.0044	0.0184	I	PE	This Paper
48213.76563	45401	-0.0037	0.0197	I	PE	Maceroni & van't Veer (1994)
48214.73011	45404	-0.0037	0.0197	I	PE	Maceroni & van't Veer (1994)
48215.85566	45407.5	-0.0034	0.0200	II	PE	Maceroni & van't Veer (1994)
48216.81983	45410.5	-0.0037	0.0197	II	PE	Maceroni & van't Veer (1994)
48217.78432	45413.5	-0.0037	0.0197	II	PE	Maceroni & van't Veer (1994)
48218.58805	45416	-0.0037	0.0197	I	PE	Maceroni & van't Veer (1994)
48262.3127	45552	-0.0026	0.0209	I	PE	This Paper
48268.2594	45570.5	-0.0036	0.0200	II	PE	This Paper
48277.2616	45598.5	-0.0033	0.0203	II	PE	This Paper
48290.282	45639	-0.0034	0.0201	I	CCD	Paschke (1992a)
48637.338	46718.5	-0.0026	0.0216	II	CCD	Paschke (1992a)
48646.3410	46746.5	-0.0015	0.0227	II	PE	This Paper
48654.2169	46771	-0.0023	0.0220	I	PE	This Paper
48934.564	47643	0.0001	0.0249	I	CCD	Paschke (1992b)
48935.5275	47646	-0.0008	0.0239	I	PE	This Paper
48952.4061	47698.5	-0.0008	0.0240	II	PE	This Paper
48978.2861	47779	-0.0012	0.0236	I	PE	This Paper
48980.3760	47785.5	-0.0011	0.0238	II	PE	This Paper
48987.4488	47807.5	-0.0012	0.0237	II	PE	This Paper
48993.3960	47826	-0.0017	0.0232	I	PE	This Paper
50098.3840	51263	0.0039	0.0309	I	CCD	Agerer & Hubscher (1996)
50113.3321	51309.5	0.0024	0.0294	II	CCD	Agerer & Hubscher (1996)

^aThe times of minima marked in asterisk were determined in this paper from the original observations by the method of Kwee and van Woerden (1956).

^{b,c}The (O-C) values were calculated with Equation (1) and the linear term of Equation (2), respectively.

third column of Table 2. As seen in Fig. 1, the (O-C) residuals for visual timings between about JD 2440000 and JD 2445000 show a large scatter of $\sim 0^d.03$. This scatter can be seen even in the very short time interval of ~ 40 days. It seems implausible that these could reflect real effects in such a short time interval. The scatters of the visual timings are strongly influenced by those of a relatively small number of estimates. Most of the visual minima and some photographic timings were then excluded from further analysis, although certain earlier minima (seven visual and three photographic) from before 1930 were included in order to provide a longer time base.

The scatters of the photoelectric minima in Fig. 1 are generally within about $0^d.005$, which is rather large for pho-

toelectric observations. This scatter, as discussed by Maceroni & van't Veer (1994), may result from apparent phase shifts of the real conjunctions due to asymmetric eclipse minima (van't Veer 1973; Kim 1992; Maceroni & van't Veer 1994). We note, however, that such a scatter would not affect the general long-term pattern of period variation, as evidenced in Fig. 1. Assuming that the difference in scatters of visual (including some photographic) and photoelectric minima are largely due to measuring uncertainties, it can be used as a measure of relative timing uncertainties. According to the ratio of inversely squared values of each scatters for visual and photoelectric minima, weights of 1 for the former and of 36 for the latter were assigned and used in subsequent calculations.

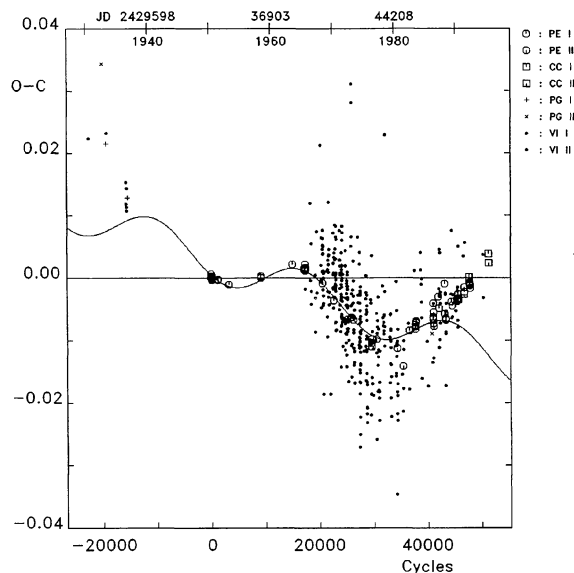


FIG. 1. (O-C) diagram of YY Eri constructed with Eq. (1). The continuous curve is drawn with the sine ephemeris of Kim (1992). The recent times of minimum lights have apparently deviated from the curve.

A generally sinusoidal character to the (O-C) trend is clear in Fig. 1. The continuous curve denotes the sinusoidal form derived by Kim (1992), which apparently does not fit too well both earlier and more recent minima, as pointed out by Maceroni & van't Veer (1994). Systematic deviations from the derived sinusoidal fit might be caused by some additional effect. Alternatively, the (O-C) variations might be seen in terms of additive abrupt period changes. In the first case some summation of an upward parabolic and sine curves would still represent the (O-C) variation. We therefore consider three possible mechanisms: (1) abrupt period changes due to irregular mass motions in the system, (2) a light time effect due to a third body together with mass transfer, or (3) a cyclic magnetic activity modulation of one or both component stars with mass transfer. For a secular period increase, mass transfer should be from the less to the more massive star. We shall examine these mechanisms one by one in the following sections.

3. ABRUPT CHANGES

Consider the (O-C) diagram in Fig. 1 in terms of abrupt period changes. The diagram is redrawn in Fig. 2 with the minima listed in Table 2. Period jumps may have occurred five times within an interval of 60 years between early 1930 and early 1990. Between these jumps the period is taken to have remained constant. Such a combination of six constant period intervals have been computed individually by the method of linear least-squares, and they are listed in Table 3, and drawn as lines in Fig. 2.

In Table 3, the second column denotes the number of occurrences of light minimum during the time interval of the first column. The initial epoch and period for each interval are given, with their probable errors in the third and fourth

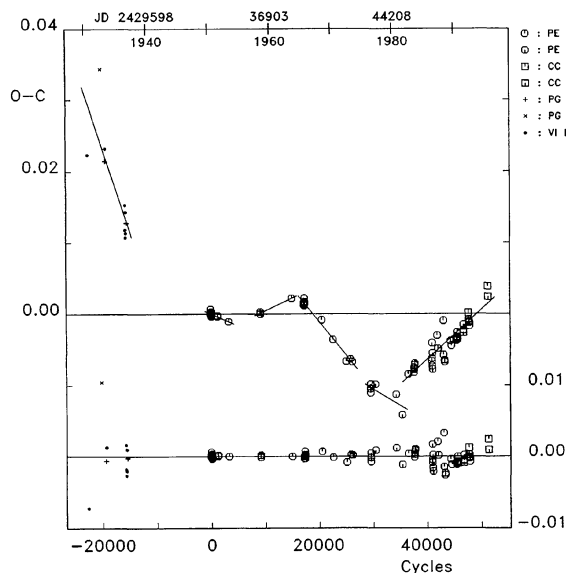


FIG. 2. (O-C) diagram of YY Eri constructed with Eq. (1). The diagram shows that the period variation of YY Eri could be interpreted as consequence of a series of the five abrupt changes of the period. Each of the lines expresses the different orbital periods listed in Table 3. The (O-C) residuals in lower part of the figure were calculated separately with the ephemerides listed in Table 3.

columns, respectively. In the lower part of Fig. 2 are plotted the (O-C) residuals, calculated using the ephemerides listed in Table 3.

Abrupt period changes for YY Eri system could be produced by anisotropic mass ejections from one (or both) component(s) (Huang 1963). However, no additional supporting evidence has been reported so far (e.g., detections of high velocity ejecting gases). As seen in Table 3, the abrupt period changes seem to have occurred repetitively in the pattern of two period increases and a subsequent decrease. This might be an indication of sinusoidal variations rather than real abrupt changes of period due to sudden mass ejections.

4. MASS TRANSFER

Our inability to explain the (O-C) curve in terms of a simple light time effect could be overcome if a quadratic term was introduced in addition to the basic sine term: The values for the quadratic term in Eqs. (2) and (3) (to be discussed later) are listed in Tables 4 and 5, respectively.

As shown in Figs. 3 and 5, an upward parabolic increase of period of YY Eri is apparent, which would imply secular mass transfer from the less (hereafter secondary) to the more massive (hereafter primary) stars. If the mass and angular momentum of the system are assumed to be conserved, then the mass transfer rate \dot{m} could be derived from a well known formula [e.g., Eqs. (4.1) and (4.2) in Pringle (1975)] as listed in Tables 4 and 5. In our calculation we used the individual masses ($m_p = 1.3 M_\odot$, $m_s = 0.5 M_\odot$) published in Paper I. The calculation indicates that gaseous matter emerging from the secondary would have to be transferred to the primary at a rate of $1.7-1.9 \times 10^{-8} M_\odot/\text{yr}$.

TABLE 3. Abrupt period jumps of YY Eri.

Interval (yr)	No. of Min. Times	Initial Epoch (JD 2400000+)	Period (day)	Period Difference (second)
1931.0 - 1937.3	10	26334.37 ± 72	0.321494 ± 128	+0.17
1950.8 - 1953.9	17	33580.548 ± 46	0.321496 ± 49	+0.09
1959.0 - 1964.1	6	36540.885 ± 75	0.321497 ± 31	-0.15
1966.0 - 1974.1	15	39120.251 ± 55	0.3214953 ± 116	+0.06
1977.0 - 1982.2	7	43118.687 ± 77	0.321496 ± 27	+0.07
1983.1 - 1993.0	26	45356.945 ± 61	0.3214969 ± 81	

In principle, the continuous mass transfer, suggested in YY Eri system, could produce a permanent bright hot spot on the surface of the mass gaining primary star. This hot spot could be seen more clearly near 0.25 phase because of the Coriolis force involved. However, there might be some difficulties in detecting the hot spot because real situations may be more complicated due to the possible existence of cool spots (Eaton 1986; Müyesseröglü *et al.* 1990). Recent discussions on the light curves and spectroscopic Doppler imaging of YY Eri system by Maceroni *et al.* (1994) show such complication. Another observable for the mass transfer may be the polarization features which have to be variable with phase. Polarimetric observations of YY Eri by Oshchepkov (1973) could be a good evidence of the mass transfer. He found that the polarization maximum occurs at 0.25 phase.

TABLE 4. The fitted parameters for Eq. (2) and mass transfer rate of YY Eri system.

Model Parameter	Final Values	Unit
T_0	HJD 2433617.5242(12)	day
P	0.32149560(4)	day
K	0.0045(16)	day
ω	0.01048(62)	deg/ P
ω_0	280.3(22.9)	deg
A	$8.73(84) \times 10^{-12}$	day
χ^2	0.44	
P_{mod}	30.2(1.8)	yr
\dot{m}	1.7×10^{-8}	m_{\odot}/yr

5. THIRD-BODY INTERPRETATION

A reasonable fit to the (O–C) curve is obtained by introducing a quadratic term to the sinusoidal ephemeris, as

$$C = T_0 + PE + AE^2 + K \sin(\omega E + \omega_0), \quad (2)$$

where the quadratic term produces the secular period increase. Equation can be solved iteratively using a Levenberg–Marquardt technique (Press *et al.* 1989). The solution is listed in Table 4 where the error measure χ^2 is given in the seventh row. The O–C values obtained by the linear

TABLE 5. The fitted parameters for the light-time orbit and mass transfer rate of YY Eri system.

Model Parameter	Final Values	Unit
T_0	HJD 2433617.5229(10)	day
P	0.32149566(3)	day
$a \sin i$	$1.41(33) \times 10^8$	km
ω	149.9(12.9)	deg
e	0.49(37)	
n	0.000481(21)	rad/day
T	HJD2427419(715)	day
A	$9.83(71) \times 10^{-12}$	day
χ^2	0.17	
P_3	35.7(1.6)	yr
K	0.00494	day
$f(m)$	0.00066	m_{\odot}
m_3		m_{\odot}
$i(90^\circ)$	0.13	m_{\odot}
$i(60^\circ)$	0.16	m_{\odot}
$i(30^\circ)$	0.28	m_{\odot}
\dot{m}	1.9×10^{-8}	m_{\odot}/yr

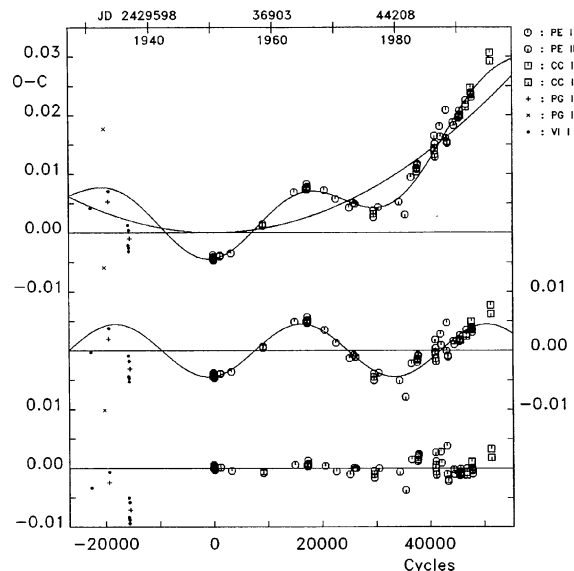


FIG. 3. (O-C) diagram of YY Eri constructed with the light elements in Table 4. The sinusoidal and quadratic curves in the upper part represent the full contribution and the quadratic term of Eq. (2), respectively. In the middle the (O-C) residuals after subtracting the quadratic term were plotted. The sinusoidal curve was drawn with only sine term in Eq. (2) with the parameters in Table 4. In the lowest there plotted the (O-C) residuals after the subtraction of all the terms in Eq. (2).

light elements in Table 4 were given in the fourth column of Table 2 and drawn in Fig. 3 together with nonlinear contributions corresponding to the fitted parameters.

In regarding a third body in the YY Eri system as the

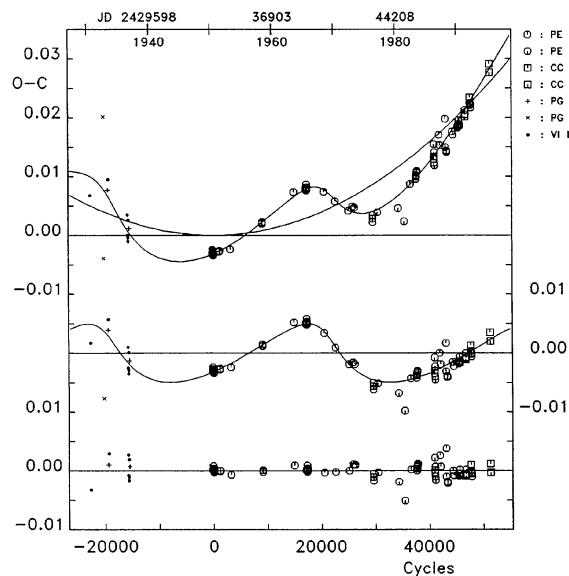


FIG. 4. (O-C) diagram of YY Eri constructed with the light elements in Table 5. The sinusoidal and quadratic curves in the upper part represent the full contribution and the quadratic term of Eq. (3), respectively. In the middle the (O-C) residuals after subtracting the quadratic term were plotted. The sinusoidal curve was drawn with the parameters for the theoretical light-time orbit in Table 5. In the lowest there plotted the (O-C) residuals after the subtraction of all the terms in Eq. (3).

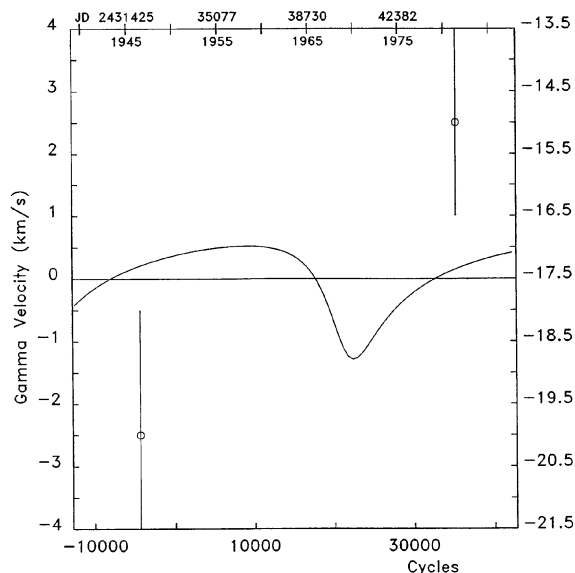


FIG. 5. γ velocity of YY Eri at different epochs (Struve 1947; Nesci *et al.* 1986). The continuous curve is the radial velocity curve corresponding to the light-time orbit in Table 5, with a zero line arbitrarily adjusted to $\gamma_0 = -17.5 \text{ km s}^{-1}$.

cause of the (O-C) variation, it is better to use a general light time ephemeris (Irwin 1952, 1959) rather than a sine curve, which is a special form ($e=0$) of the light-time ephemeris given by

$$C = T_0 + PE + AE^2 + \tau, \quad (3)$$

where τ is the light-time effect due to the third body. A more generalized treatment of Eq. (3) would involve a differential corrections procedure to determine eight unknown parameters (Irwin 1959). Initial parameters for the Levenberg-Marquardt method used to solve for the orbit giving rise to the light-time effect were obtained from Kim's (1992) values, and the initial coefficient A in Eq. (3) graphically estimated. The final solutions are listed in Table 5, together with physically related parameters. The O-C residuals with respect to the linear part of the light-time equation are plotted in Fig. 4 together with nonlinear prediction for the eclipse timings corresponding to the elements of Table 5.

The value n in Table 5 denotes the Keplerian mean motion of an elliptical orbit of the mass center of the eclipsing pair. K , in the eleventh row, is the amplitude of the light time τ , expressed as $K = (\tau_{\max} - \tau_{\min})/2$. The other parameters in Table 5 are self-explanatory. The derived values for the orbital elements of the assumed third-body are quite close to those of Kim (1992). The masses of the third body, as expected from the small amplitude of K and thus small mass function, range from $0.13 M_{\odot}$ to $0.28 M_{\odot}$ for the inclination range 90° to 30° . In the calculation the total mass of $1.8 M_{\odot}$ for the eclipsing pair was used (Paper I).

The semiamplitude of the radial velocity of the center of mass of the eclipsing pair, relative to the mass center of the triple system, turns out to be 0.90 km/s , which is too small for present-day spectroscopic observations reliably to resolve. Struve (1947) found -20 km/s as the system velocity

of YY Eri, but Nesci *et al.* (1986) derived -15 km/s from their own observations. It is not certain whether the difference between these solutions is due to perturbations from a third body, or observational uncertainties. The difference is large, however, compared to the 0.05 km/s calculated with the orbital parameters of Table 5. This situation is illustrated in Fig. 5, where the γ velocity of zero corresponds to -17.5 km/s.

The third-body masses listed in Table 5 are quite small, so a third-body spectrum would not be expected. YY Eri is $50\text{--}70$ pc far from our Sun (Dworak 1973; Rucinski 1983; Paper I). The semimajor axis ($a \sin i$) of the center of mass of the close pair about the system center is 0.94 AU. The corresponding angular size, at a distance of 50 pc, would be $0''.2\text{--}0''.04$ for $i=90^\circ\text{--}30^\circ$, and at 70 pc, $0''.013\text{--}0''.027$. Astrometric observations at resolutions substantially better than these would be needed to establish whether or not the suggested third body exists.

6. MAGNETIC ACTIVITY INTERPRETATION

As an alternative explanation for cyclic changes of orbital period of YY Eri, Applegate's (1992) model deserves attention. According to this theory, strong magnetic activities below the surface of one or both stars play major roles in producing period variations. Changes in the magnetic field distribution in an active star during its magnetic cycle change the distribution of angular momentum. This sequentially yields changes to the quadrupole moment, resulting in changes to the star's oblateness and radial differential rotation. Variations in shape of the star would be gravitationally coupled to the orbit, modulating the orbital period. In addition, the rms luminosity of the active star would be variable with the same period as that of the orbital period modulation.

Using the modulation period and amplitude listed in Table 4 and adopting the absolute dimensions of YY Eri from Paper I, the variations of parameters needed to change the orbital period for YY Eri by specified amounts can be obtained from the formulas given by Applegate (1992).

Our calculations have been applied to both components, because we do not know, at present, anything about the relative magnetic activities of the components, although it was proposed by Mullan (1975) that the more massive components of W UMa systems would preferentially manifest starspots and thus magnetic activity (see also Eaton 1986).

The results of our calculations are listed in Table 6, where ΔP ($\Delta P/P$), ΔJ , I_s , $\Delta\Omega$ ($\Delta\Omega/\Omega$), ΔE , ΔL_{rms} , and B denote amplitude of orbital period modulation, angular momentum transfer, moment of inertia of the convective shell, variable part of the differential rotation, energy needed to transfer the angular momentum, rms luminosity variation, and mean subsurface magnetic intensity, respectively. The mass of the convective shell is assumed to be one tenth of the mass of the active star, as suggested by Applegate (1992). Our results imply that Applegate's mechanism could explain the observed period modulations of YY Eri and that both stars could play a role in this.

The luminosity changes (ΔL_{rms}) for both stars in Table 6 can be converted to magnitudes via Pogson's equation, thus:

TABLE 6. The model parameters for the magnetic activities of YY Eri system.

Model	Massive	Less Massive	Unit
Parameter	Cool Star	Hot Star	
ΔP	0.07	0.07	s
$\Delta P/P$	2.56×10^{-6}	2.56×10^{-6}	
ΔJ	8.96×10^{46}	4.93×10^{46}	gcm^2/s
I_s	1.16×10^{54}	1.84×10^{53}	gcm^2
$\Delta\Omega$	7.75×10^{-8}	2.67×10^{-7}	s^{-1}
$\Delta\Omega/\Omega$	3.43×10^{-4}	1.18×10^{-3}	
ΔE	1.39×10^{40}	2.64×10^{40}	erg
ΔL_{rms}	4.57×10^{31}	8.67×10^{31}	erg
	0.012	0.023	L_\odot
	0.012	0.046	L_s
B	5.75	8.24	kG

$$\Delta m = -2.5 \log \left(1 \pm \frac{\Delta L_{rms}}{L_p + L_s} \right), \quad (4)$$

where L_p and L_s denote bolometric luminosities for the cool primary and hot secondary stars, respectively. Here we have used the luminosities of Paper I ($L_p = 1.05L_\odot$ and $L_s = 0.54L_\odot$). With Eq. (4) the bolometric magnitude difference Δm relative to the mean light level of YY Eri come out as $\pm 0^m.009$ and $\pm 0^m.016$, with the assumption of primary and secondary as magnetically active star, respectively. These values may be regarded as upper limits because some of the transferred energy is expected to be uniformly dissipated in the boundary between the radiative interior and the convective shell.

In order to look for any long-term light variations of YY Eri, we collected eleven photoelectric light curves published so far. From these, each of the light levels of four characteristic phases (Min I, the minimum light at midpoint for primary eclipse; Min II, for secondary eclipse; Max I, the maximum light following the primary eclipse; Max II, following the secondary eclipse) was measured in both B and V spectral ranges. Differences were then worked out as Min I–Min II, Max I–Max II, Max I–Min I, Max I–Min II, Max II–Min I, Max II–Min II, and (Min I–Min II)–(Max I–Max II), respectively. These have been listed for V and $(B-V)$ in Table 7.

In Table 7 the epochs in the first column were calculated,

TABLE 7. Long-term light variations of YY Eri system.*

cycles	year	M1-M2 ^a	A1-A2 ^b	A1-M1 ^c	A1-M2 ^d	A2-M1 ^e	A2-M2 ^f	A12-M12 ^g	Note**
93	1951.0	0.072	0.000	-0.693	-0.621	-0.693	-0.621	0.072	1
		-0.005	0.004	-0.023	-0.028	-0.027	-0.032	-0.009	
774	1951.6	0.076	-0.011	-0.699	-0.623	-0.688	-0.612	0.087	2
		-0.036	-0.014	-0.003	-0.039	0.011	-0.025	-0.022	
9068	1958.9	0.067	-0.019	-0.710	-0.643	-0.691	-0.624	0.086	3
		0.011	0.007	-0.021	-0.010	-0.028	-0.017	0.004	
17220	1966.2	0.090	-0.008	-0.735	-0.645	-0.727	-0.637	0.098	4
		0.038	0.008	-0.050	-0.012	-0.058	-0.020	0.030	
29517	1976.9	0.088	-0.004	-0.720	-0.632	-0.716	-0.628	0.092	5
		-	-	-	-	-	-	-	
36540	1983.1	0.099	-0.007	-0.721	-0.622	-0.714	-0.615	0.106	6
		-0.018	0.016	-0.021	-0.039	-0.037	-0.055	-0.034	
38152	1984.5	0.150	0.023	-0.750	-0.600	-0.773	-0.623	0.127	7
		0.006	-0.021	-0.034	-0.028	-0.013	-0.007	0.027	
43279	1989.0	0.090	0.016	-0.663	-0.573	-0.679	-0.589	0.074	7
		0.023	0.008	-0.049	-0.026	-0.057	-0.034	0.015	
44968	1990.5	0.048	-0.014	-0.692	-0.644	-0.678	-0.630	0.062	8
		-0.003	-0.003	-0.038	-0.041	-0.035	-0.038	0.000	
45571	1991.0	0.106	0.000	-0.710	-0.604	-0.710	-0.604	0.106	7
		-0.038	0.006	0.001	-0.037	-0.005	-0.043	-0.044	
47734	1992.9	0.076	0.000	-0.696	-0.620	-0.696	-0.620	0.076	7
		-0.069	0.000	-0.167	-0.236	-0.167	-0.236	-0.069	
mean		0.087	-0.002	-0.708	-0.621	-0.706	-0.618	0.090	
		(0.026)	(0.012)	(0.024)	(0.022)	(0.027)	(0.013)	(0.019)	
		-0.009	0.001	-0.040	-0.050	-0.042	-0.051	-0.010	
		(0.032)	(0.011)	(0.048)	(0.066)	(0.049)	(0.067)	(0.032)	

* The 1st and 2nd rows at each epoch denote values for V and $(B-V)$, respectively.

**¹Cillié (1951), ²Huruhata *et al.* (1953), ³the Pugathofers (1960), ⁴Bhattacharyya (1967),

⁵Eaton (1976), ⁶Budding (1983), ⁷This paper, ⁸Maceroni & van't Veer (1994)

^aM1-M2=Min I-Min II, ^bA1-A2=Max I-Max II, ^cA1-M1=Max I-Min I, ^dA1-M2=Max I-Min II,

^eA2-M1=Max II-Min I, ^fA2-M2=Max II-Min II, ^gA12-M12=(Max I-Max II)-(Min I-Min II).

using the light elements in Table 4, by averaging start and end times. Corresponding calendar dates are in the second column. The final two values of each column, from the third to the ninth, represent mean values of each quantity for V and $(B-V)$, respectively, with their standard deviations in parentheses.

The apparent light and color variations listed in Table 7 are remarkable. The standard deviations relative to the mean value of each data set range from $0^m.012$ to $0^m.027$ for (V) , while those for $B-V$ vary over $0^m.011$ and $0^m.067$. To find any sinusoidal behavior in these light and color variations each of data sets in Table 7 was separately fitted to the following equation:

$$m = m_o + K \sin(\omega E + \omega_o). \quad (5)$$

In these calculations ω is fixed by adopting its value from Table 4. The final results for each data set are listed in Table 8 with their standard errors. Each data set is plotted in Fig. 6. The continuous curves in this figure were drawn using Eq. (5).

In Fig. 6 a sinusoidal variation of (Max II-Min II) for V light can be seen. The value of (Max II-Min I) for V light also seems to vary in a more or less sinusoidal way. But all

other differences, including those for the $(B-V)$ colors, show no clear sinusoidal pattern. According to Applegate's (1992) theory, if either of the stars in YY Eri is magnetically active, changes to the mean bolometric luminosity occur globally, in response to the magnetic cycle. Thus if no local photospheric inhomogeneities exist, then the light and color variations for each data set in Table 7 except those for (Max I-Max II) should be perfectly sinusoidal.

Why do we find only the variation of (Max II-Min II) to be nearly sinusoidal? We can provide a general explanatory scenario if we suppose the primary star to be magnetically active, and some local inhomogeneities on its surface are seen at $0^p.25$ (corresponding to Max I), but not at $0^p.75$ (Max II). In this case, the light for Max II would change in accordance with the magnetic cycle, while the light changes for Max I would be more complicated, due to the local inhomogeneities. The supposed constant light from the secondary star could be used as a reference. In fact, the light from YY Eri at $0^p.5$ (Min II) comes mainly from the secondary's averted hemisphere, together with some unclipped portions of the primary star. The light for Min II would then be more stable than those for other phases. In this way, the variations

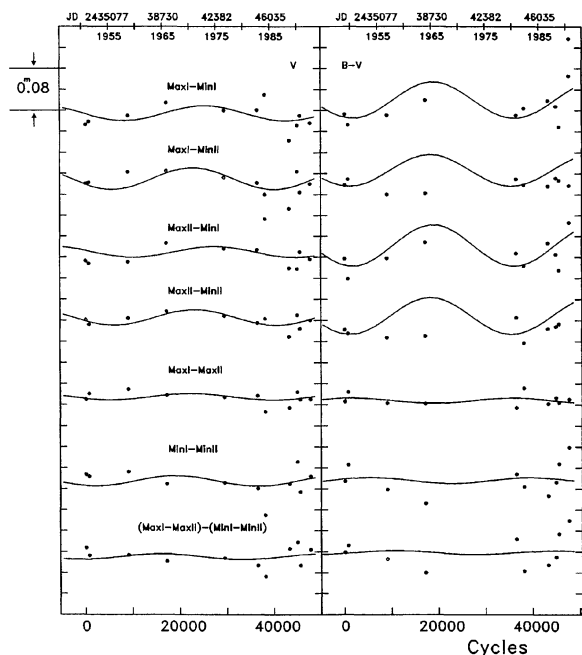


FIG. 6. The variation of the V light and $(B-V)$ color curves of YY Eri at different characteristic phases ($0^{\text{P}}0$, $0^{\text{P}}25$, $0^{\text{P}}50$, $0^{\text{P}}75$). The continuous curves are drawn with Eq. (5) using the parameters in Table 8. It is interesting to see that the variation of $(\text{Max II}-\text{Min II})$ in V light is nearly sinusoidal.

of $(\text{Max II}-\text{Min II})$ measure, more or less, the global changes of the rms luminosity. Local surface inhomogeneities at $0^{\text{P}}25$ could be in keeping with Struve's (1947) spectroscopic and Oschepkov's (1973) polarimetric observations.

The amplitude of the sinusoidal pattern of $(\text{Max II}-\text{Min II})$ in V is $0^{\text{m}}015$, which is close to the rms luminosity change of $0^{\text{m}}009$ for the primary star calculated with the Applegate theory. If so, the magnetically active star in YY Eri system could be that primary star. The $30^{\text{P}}2$ period modulation of YY Eri would then be the period of its magnetic activity cycle.

7. SUMMARY AND DISCUSSION

With the foregoing analysis of times of minima of YY Eri, we have considered three plausible mechanisms to explain the nature of the apparent period changes of YY Eri: (1) abrupt changes due to occasional mass ejections in the system, (2) a light-time effect due to a hypothetical third body superposing on a continuous transfer of mass from secondary to primary, (3) a cyclic magnetic activity modulation of the primary star combined with a continuous mass transfer. Among these ideas, at present, the magnetic activity interpretation seems more plausible. No evidence of anisotropic mass ejections from YY Eri, which would result in the observed abrupt period changes, has been reported so far. As to the third-body hypothesis, it is not certain whether the difference in γ velocities of Struve (1947) and Nesci *et al.* (1986) is due to perturbations from a third body, or observational uncertainties. However, the light variations of Max

TABLE 8. Fitted parameters for Eq. (5).

		m_o	K	ω_o
		(mag)	(mag)	(deg)
Min I	- Min II	0.085(24)	-0.010(36)	249(190)
		-0.006(30)	0.006(45)	214(45)
Max I	- Max II	-0.005(11)	-0.006(18)	215(140)
		0.002(10)	-0.005(14)	253(170)
Max I	- Min I	-0.715(21)	0.014(31)	4(115)
		-0.050(39)	-0.035(55)	251(92)
Max I	- Min II	-0.630(18)	-0.021(28)	210(67)
		-0.056(59)	-0.030(83)	438(162)
Max II	- Min I	-0.710(25)	0.010(35)	342(204)
		-0.052(39)	-0.039(54)	252(79)
Max II	- Min II	-0.625(11)	-0.015(16)	206(55)
		-0.058(58)	-0.035(81)	437(137)
Max 12	- Min 12*	0.089(17)	0.005(24)	101(278)
		-0.008(30)	-0.004(43)	158(314)

*Max 12-Min 12 = $(\text{Max I}-\text{Max II})-(\text{Min I}-\text{Min II})$

II-Min II seem to have followed the behavior of period variation for YY Eri, which Applegate's magnetic activity model requires.

In our magnetic activity picture the primary is taken to be the predominantly magnetically active star producing the observed period changes and the global light variations. The photosphere of the primary seen at $0^{\text{P}}25$ is different from that at $0^{\text{P}}75$ in order to explain the whole of the observed light variations of YY Eri. Such local inhomogeneities would have to have existed within at least the past ~ 65 years.

In addition, we expect gaseous material from the secondary is transferring to the primary at a rate of about $1.7-1.9 \times 10^{-8} M_{\odot}/\text{yr}$. This mass transfer process could fit in with the pre-Algol scenario referred to in Paper I.

However, our picture explaining the period changes of YY Eri still has several problems. First, according to the Applegate's model the color variations of Max II-Min II should follow the same sinusoidal pattern as monochromatic ones. But we do not see the color variation in Fig. 6. Second, the deduced mean subsurface magnetic intensity of ~ 6 kG is remarkably strong. Thus the binary system should exhibit some observational effects supporting such a strong magnetic field. However, there is no agreement with the existence of dark spots (Eaton 1986; Müyesseroglu *et al.* 1990; Maceroni *et al.* 1994). The x-ray flux from YY Eri is rela-

tively weak (Crudace & Dupree 1984). They failed to detect any radio emissions (Beasley *et al.* 1993). Third, as seen in the lowest part of Fig. 5, there exist small and regular oscillations in the (O–C) residuals after the subtraction of all the terms in Eq. (2). These observed facts suggest that a third-body interpretation cannot be ruled out by the present data.

On balance, the supporting evidence of the luminosity variations argues in favor of a magnetodynamic explanation. But we should now seek additional evidence for magnetodynamic activity (e.g., cyclic effects in emission lines, or maculation effects in the photometry, or radio or other EUVE, x-ray data), or other third-body effects (e.g., cyclic variations

of γ velocity or third-body spectrum in high resolution spectroscopy, or detection of any third light in photometry, or cyclic position changes in astrometry) in order to resolve the issue more firmly.

We sincerely appreciate the precious comments and suggestions from the anonymous referee. We thank Dr. C. Han for carefully reading our manuscript. This work is supported in part by NON DIRECTED RESEARCH, Korea Research Foundation and in part by grant (BSRI-96-5426) from Ministry of Education, Korea. Two of us (C.H.K. & J.H.J.) acknowledge the financial support.

REFERENCES

- Agerer, F., & Hubscher, J. 1996, IBVS, 4383
 Applegate, J. H. 1992, ApJ, 385, 621
 Batten, A. H. 1973, Binary and Multiple System of Stars (Pergamon, Oxford), Chap. 4
 Beasley, A. S., Ball, L. T., Budding, E., Slee, O. B., & Stewart, R. T. 1993, AJ, 106, 1656
 Bhattacharyya, J. C. 1967, Kodaikanal Observatory Bull. Ser. No. 181
 Binnendijk, L. 1965, AJ, 65, 358
 Binnendijk, L. 1970, Vistas Astron., 12, 217
 Bodokia, V. M. 1938, Bull. Ap. Obs. Abastumani, 3, 9
 Budding, E. 1983, IBVS, 2300
 Budding, E., Kim, C.-H., Demircan, O., Müyesseröglü, Z., Saijo, K., & Banks, T. 1997, Ap&SS, 246, 229
 Cillié, G. G. 1951, Harvard Coll. Obs. Bull., 920, 41
 Crudace, R. G., & Dupree A. K. 1984, ApJ, 277, 263
 Demircan, O., Derman, E., Akalin, A., Selam, S., & Müyesseröglü, Z. 1994, MNRAS, 267, 19
 Diethelm, R. 1982, BBSAG Bull. 53
 Dworak, T. Z. 1973, IBVS, 846
 Eaton, J.A. 1986, Acta Astron., 36, 79
 Ebersberger, J., Kizilirmak, A., & Pohl, E. 1978, IBVS, 1449
 Hobart, M. A., Peña, J. H., Peniche, R., Ríos-Herrera, M., Ríos-Berúmen, M., Rodríguez, E., & López-Cruz, O. 1993, IBVS, 3935
 Hobart, M. A., Peña, J. H., Peniche, R., Rodríguez, E., Garrido, R., Ríos-Berúmen, M., Ríos-Herrera, M., & López-Cruz, O. 1994, Revista Mexicana de Astronomía y Astrofísica, 28, 111
 Huang, S. S. 1963, ApJ, 138, 471
 Huruata, M., Dambara, T., & Kitamura, M. 1953, Tokyo Ann. Second Ser., 3, 227
 Irwin, J. B. 1952, ApJ, 116, 211
 Irwin, J. B. 1959, AJ, 64, 149
 Jensch, A. 1934, AN, 251, 329
 Kalimeris, A., Rovithis-Livanou, H., Rovithis, P., Oprescu, G., Dumitrescu, A., & Suran, M. D. 1994, A&Ap, 291, 765
 Kim, C.H. 1992, in Evolutionary Processes in Interacting Binary Stars, edited by Y. Kondo, R. F. Sistero, and R. S. Polidan (Kluwer, Dordrecht), p. 383
 Kizilirmak, A., & Pohl, E. 1971, IBVS, 530
 Kizilirmak, A., & Pohl, E. 1974, IBVS, 937
 Kwee, K. K. 1958, BAN, 14, 131
 Kwee, K. K., & van Woerden, H. 1956, BAN, 12, 327
 Lause, F. 1934, AN, 263, 115
 Maceroni, C., & van't Veer, F. 1994, A&A, 289, 871
 Maceroni, C., Vilhu, O., van't Veer, F., Van Hamme, W. 1994, A&A, 288, 529
 Mullan, B. J. 1975, ApJ, 198, 563
 Müyesseröglü, Z., Demircan, O., Derman, E., & Selam, S. 1990, in Active Close Binaries, edited by C. Ibanoglu (Kluwer, Dordrecht), p. 277
 Nesci, R., Maceroni, C., Milano, L., & Russo, G. 1986, A&A, 159, 142
 Oshchepkov, V. A. 1973, IBVS, 782
 Paschke, A. 1992a, BBSAG Bull. 100
 Paschke, A. 1992b, BBSAG Bull. 102
 Pohl, E., & Kizilirmak, A. 1966, A. N., 289 (H4)
 Pohl, E., & Kizilirmak, A. 1970, IBVS, 456
 Prager, R. 1941, Ann. Harvard College Obs., 111
 Press, W., Flannery, B. P., Teukolsky, S. A., & Vetterling, W. T. 1989, Numerical Recipes (Cambridge University Press, Cambridge), Chap. 14
 Pringle, J. E. 1975, MNRAS, 170, 633
 Purgathofer, A., & Purgathofer, I. 1960, Mitt. Wien, 10, 195
 Rucinski, S. M. 1983, A&A, 127, 84
 Skillman, D. R. 1982, JAAVSO, 11, 57
 Strauss, F. M. 1976, PASP, 88, 531
 Struve, O. 1947, ApJ, 106, 92
 Tremblot, R. 1933, Une étoile Variable à Eclipses de Courte Periode CR Paris, 196, 1162
 van't Veer, F. 1973, A&A, 26, 357
 Wood, F. B. 1950, ApJ, 112, 196